

## Metastable *vs.* unstable growth in the subsurface ordering dynamics of $\text{Cu}_3\text{Au}(001)$

H. REICHERT<sup>1</sup>, H. DOSCH<sup>1</sup>, P. J. ENG<sup>2</sup> and I. K. ROBINSON<sup>2</sup>

<sup>1</sup> *Max-Planck-Institut für Metallforschung - Heisenbergstr. 1, 70569 Stuttgart, Germany*

<sup>2</sup> *University of Illinois at Urbana-Champaign - Urbana, Illinois 61801, USA*

(received 20 September 2000; accepted in final form 18 December 2000)

PACS. 05.70.Ln – Nonequilibrium and irreversible thermodynamics.

PACS. 61.10.Eq – X-ray scattering (including small-angle scattering).

PACS. 64.60.My – Metastable phases.

**Abstract.** – A surface-sensitive X-ray line shape analysis of the ordering process in  $\text{Cu}_3\text{Au}(001)$  has been performed following a rapid temperature quench from the disordered phase into the ordered phase. We study the temporal evolution of ordered domains in the subsurface region. We find distinct and anisotropic antiphase domain patterns in the unstable and metastable growth mode. This leads to rather unusual surface-induced coarsening schemes.

Nonequilibrium thermodynamic properties of first-order phase transformations are of fundamental importance for a detailed understanding of kinetic phenomena in nature and technology. Thus, the growth and coarsening kinetics of (low temperature) bulk ordered phases has been the subject of numerous experimental and theoretical studies [1–4].

Within the ordered phase of  $\text{Cu}_3\text{Au}$  two fundamentally different growth modes exist (see fig. 1). The spinodal curve (SP) separates regimes associated with metastable and unstable growth kinetics [5]. Unstable (spinodal) growth starts out with homogeneous nucleation where fluctuations on all length scales are unstable, whereas metastable growth is dominated by heterogeneous nucleation at randomly distributed nucleation sites. The graphs (a) and (b) on the left side of fig. 1 show a sketch of the two growth modes in bulk systems at early time scales following a quench from the disordered into the ordered phase. Domains associated with different ordering phases are growing, thereby producing a pronounced antiphase domain pattern.

Experiments studying the early time relaxation of fluctuations after a quench into the ordered phase have unravelled a relaxation time of about 10s for  $\text{Cu}_3\text{Au}$  [6] and evidence that the boundary between the two growth regimes exhibits a smooth crossover. Medium and late stage bulk ordering kinetics in the classical coarsening regime has also been studied in detail [7, 8] showing an isotropic evolution of the ordered phase. In this coarsening stage it is not possible to distinguish between the two growth modes since the resulting antiphase domain network looks the same in each case due to the random phase and the isotropic distribution of antiphase domains boundaries. Therefore, any spinodal character in this bulk ordering process can be seen only in the very early stages of the ordering process.

Time-resolved scattering experiments have proven to be an ideal tool for probing the evolution of ordered states on different time and length scales: The temporal development of order fluctuations into domains of linear size  $\lambda$  in the early time regime is accessible at

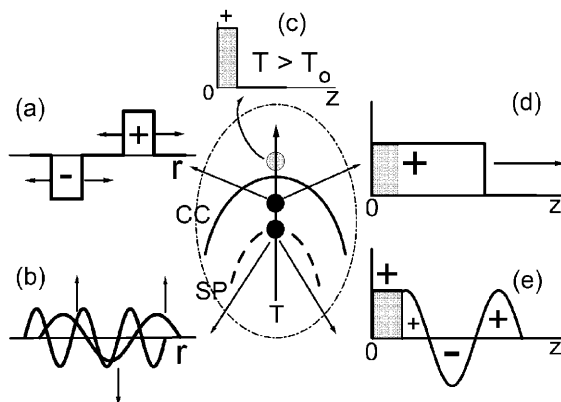


Fig. 1 – Ordering scenarios in  $\text{Cu}_3\text{Au}$ -type phase diagrams (center part). The coexistence curve (CC) separates the disordered from the ordered phase, the spinodal curve (SP) unstable from metastable growth regimes. The time evolution of the local OP components  $\Psi_i$  in real space is sketched for the bulk in the metastable (a) and unstable (b) growth regime. The upper graph (c) depicts the non-zero surface-induced OP  $\Psi_3$  in the bulk-disordered phase prior to the quenches. The time evolution of the local OP  $\Psi_3$  in the subsurface region is sketched in the metastable (d) and unstable (e) growth regime, respectively (plus and minus signs denote the phase of the OP components, for further explanations see main text).

finite momentum transfers  $q = Q - G_{hkl} = 2\pi/\lambda$  around superstructure reflection positions  $G_{hkl}$ . The time evolution of the average order parameter (OP) can be extracted from the Bragg intensities at  $q = 0$ . The domain pattern in the medium and late stage is characterized via the intensity distribution around  $G_{hkl}$ , where the lineshape and the peak width are the characteristic quantities allowing to extract the size distribution of the antiphase domains.

In this letter we apply the concept of line shape analysis to the surface of an ordering alloy: We have used surface-sensitive glancing angle diffraction to study the evolution of the domain distribution in the subsurface region of  $\text{Cu}_3\text{Au}(001)$ . By a detailed study of the time and depth dependence of all OP components of the system, we probed the dynamics of the ordering process at the surface in both growth modes and on various length scales.

$\text{Cu}_3\text{Au}$  exhibits below the order-disorder temperature  $T_0 = 663\text{ K}$  a fourfold degenerate  $L1_2$  ground state which requires a four-component OP  $\Psi = (\Psi_1, \Psi_2, \Psi_3, \Psi_4)$  with  $\Psi_1, \Psi_2, \Psi_3$  being related to ordering waves in the (100), (010), and (001) direction, respectively, and  $\Psi_4$  to the average concentration (for details, see [9]).

Close to a surface the evolution of ordered domains is strongly affected by the break of the translational symmetry. At the (001) surface it has been observed that the OP component  $\Psi_3$  (ordering waves normal to the surface) is stabilized by the Au surface segregation [9], while the in-plane OP components  $\Psi_1$  and  $\Psi_2$  are unaffected by segregation and show surface disordering [10]. Previous studies of the ordering kinetics at the  $\text{Cu}_3\text{Au}(001)$  surface have concentrated on the time evolution of the average local order (“ $q = 0$ ”) unravelling a fast temporal evolution of the average  $\Psi_3$  component in the subsurface region [11]. This is the signature of a highly anisotropic growth process in the subsurface region [12].

The objective of this study is the intriguing idea whether or not the Au surface segregation may lock the phase of normal concentration waves to  $\Psi_3(z = 0) = +1$  at the surface ( $z$  is the coordinate normal to the surface,  $z = 0$  denotes the surface). Due to this non-random and anisotropic initial growth of the OP components, we may expect antiphase domain structures

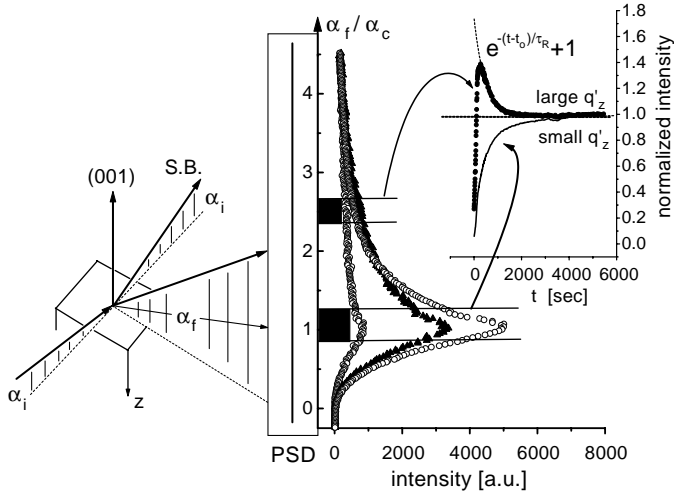


Fig. 2 – Sketch of the experimental setup: The right side shows typical intensity profiles in arbitrary units at different times on the PSD along the exit angle direction  $\alpha_f$  which corresponds in a good approximation to the  $L$  direction in reciprocal space. The time evolution of the diffracted intensities in the two exit angle ranges is also shown. The solid line is a fit to an exponential decay.

which are distinctly different in both growth modes (see the right side of fig. 1). In contrast to the situation in the bulk metastable growth at the surface (fig. 1d) starts from a single nucleus at the surface, *i.e.* the segregated layer, which is infinite in 2D. The growth front proceeds from this single 2D nucleus into the bulk without producing any antiphase domain pattern. In the case of unstable growth (fig. 1e) we expect a spectrum of ordering waves starting at the surface with the same phase producing an antiphase domain pattern on a spectrum of different length scales. Performing a detailed line shape analysis on surface Bragg reflections normal to the surface we can, thus, distinguish between an antiphase pattern produced by spinodal ordering and a single domain growing from a 2D nucleus during metastable growth. In the first case the antiphase pattern will undergo coarsening, while no such coarsening is expected for the single domain growth.

The UHV experiments have been carried out at beamline X16A at the National Synchrotron Light Source (NSLS) at the Brookhaven National Laboratory (details of the experimental procedure and the sample have been described elsewhere [9, 11]). We have used evanescent effects at grazing angles in order to tune the depth of the probing X-rays. In the evanescent scattering geometry (see fig. 2) the normal momentum transfer within the sample ( $q'_z$ ) has a large imaginary component [13] as determined by the incident ( $\alpha_i$ ) and exit angle ( $\alpha_f$ ) of the X-ray beam. By setting both angles  $\alpha_i$  and  $\alpha_f$  independently, we are able to study ordering processes at fixed scattering depths  $\Lambda = 2\pi/\text{Im}(q'_z)$  on varying length scales  $\lambda = 2\pi/\text{Re}(q'_z)$  in the subsurface regime and vice versa. The diffracted intensities have been recorded with a linear position-sensitive detector (PSD) aligned perpendicular to the surface in a grazing-angle geometry close to the critical angle of total external reflection  $\alpha_c = 0.5^\circ$  (see fig. 2). Quenches while scanning  $G_{110}$  have been performed from  $T_i = T_0 + 26$  K to  $T_f = T_0 - 20$  K which lies in the metastable growth regime for the bulk, and to  $T_f = T_0 - 30$  K which is very close to the bulk spinodal temperature  $T_{sp} = T_0 - 30$  K [6, 14, 15]. Quenches while scanning  $G_{100}$  have been started after annealing at  $T_i = T_0 + 6$  K. In the experiment a time resolution of 2 s has been achieved for recording a full diffraction profile together with a

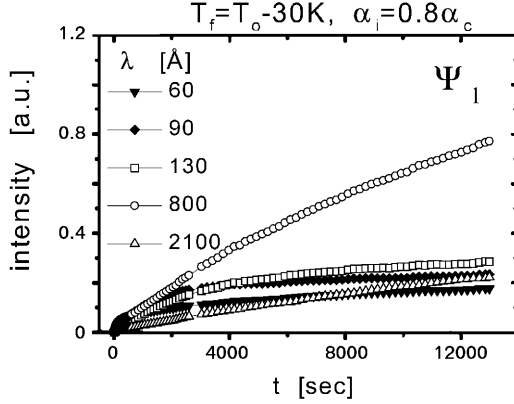


Fig. 3 – Evolution of the (100) glancing-angle intensity ( $\Psi_1$ ) in five different  $\lambda$  ranges for a quench to a final temperature  $T_f = T_0 - 30$  K in the spinodal regime.

quenching rate of 0.55 K/s to  $T_f = T_0 - \Delta T$ .

Figure 2 shows a sketch of the experimental setup together with typical diffraction profiles. By way of example, two exit angle intervals are indicated which can be converted into the associated length scale  $\lambda$  and scattering depth  $\Lambda$ . Figure 2 also depicts a typical time evolution of the scattered intensity around  $G_{110}$  for two different momentum transfer intervals (see below).

First we turn to the growth of the in-plane OP component  $\Psi_1$  ( $G_{100}$ ). Figure 3 shows the diffracted intensity in different  $\lambda$  intervals.  $\Psi_1$  does not show any particular surface behavior, especially the time evolution is bulk-like. Independent of the particular value of  $q'_z$  and the associated real space length scale  $\lambda$ , the scattered intensity is increasing monotonically. This finding is also independent of the final temperature in the quench ( $\Delta T = 10$ –30 K) and the scattering depth in the near surface region (25 Å–500 Å). Similar to the bulk case we, therefore, cannot distinguish between metastable and unstable growth regime of the in-plane order in the near surface region.

Now we turn to the time evolution of ordering waves perpendicular to the surface (“ $\Psi_3$ -waves”) as measured close to the (110) in-plane surface reflection. In a first set of measurements we have that the time dependence after a temperature quench to  $T_f = T_0 - 30$  K as observed at two different incidence angles shows a rather peculiar phenomenon depending on the choice of the length scale  $\lambda$  (fig. 4a): For large  $\lambda$  the scattered intensity increases monotonically [16]. Contrary to that, the X-ray scattering associated with small  $\lambda$  exhibits a quite unexpected and rather dramatic degree of overshooting at early times that amounts to as much as 60% of the late stage equilibrium value.

In order to rule out resolution effects in our line shape analysis of the (110) surface reflection, we have also measured the intensity profile parallel to the surface. We find that the width of the (110) surface reflection remains constant during the quenches and is, therefore, independent of the ordering process. The overshooting  $\Psi_3$ -transient is observable only within a certain regime of quench temperatures close to or below  $T_{sp}$ . Quenches to  $T_f = T_0 - 20$  K within the metastable growth regime have shown no transient  $\Psi_3$ -effects, instead we found fast relaxation on all length scales and only very small overshooting effects of less than 3% for the largest momentum transfer, *i.e.* the smallest value of  $\lambda$ , corresponding to the size of nucleating droplets for the low-temperature phase (see fig. 4b).

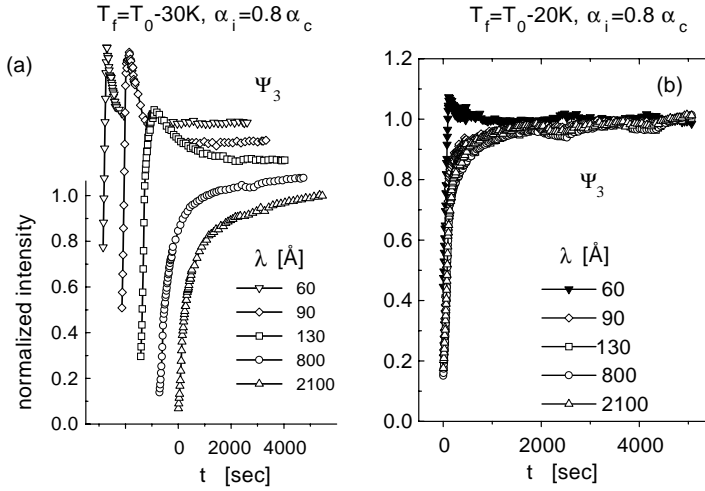


Fig. 4 – (a) Evolution of the normalized (110) glancing-angle intensity in five different  $\lambda$  ranges for a quench to a temperature  $T_f = T_0 - 30$  K in the spinodal regime for  $\alpha_i = 0.8\alpha_c$ . For clarity the curves have a constant offset along both axis. (b) Evolution of the normalized (110) glancing-angle intensity ( $\Psi_3$ ) in five different  $\lambda$  ranges for a quench to a temperature  $T_f = T_0 - 20$  K in the metastable regime.

Both the existence of overshooting only for  $\Psi_3$  and its dependence on the quench temperature imply that overshooting is associated with the antiphase pattern as produced by spinodal growth of the surface-locked  $\Psi_3$ -component. The total degree of the overshooting is given by the excess quantity

$$\epsilon(q'_z) = \int_{t_0}^{\infty} \left( \frac{I(q'_z, t)}{I(q'_z, \infty)} - 1 \right) dt,$$

where  $I(q'_z, t)$  are the observed intensities,  $I(q'_z, \infty)$  is the extrapolated equilibrium value, and  $t_0$  denotes the time at which the intensity  $I(q'_z, t)$  starts to overshoot  $I(q'_z, \infty)$  (see fig. 2). Figure 5 displays  $\epsilon(q'_z)$  for two different incidence angles associated with scattering depths

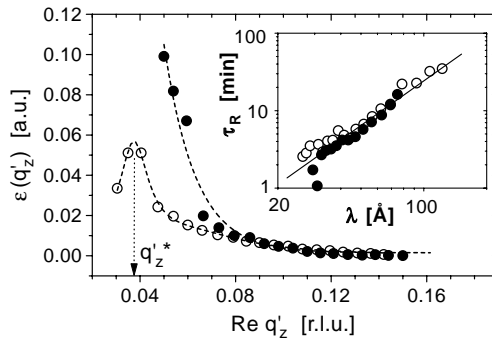


Fig. 5 – Overshooting in arbitrary units for quenches to  $T_f = T_0 - 30$  K (open circles:  $\alpha_i = 0.8\alpha_c$ ; filled circles:  $\alpha_i = 1.2\alpha_c$ ; dashed lines are guides for the eye). The inset shows the observed relaxation time  $\tau_R$  vs. length scale  $\lambda$  on a double-log plot. The straight line is the best fit giving  $\tau_R \sim \lambda^{1.92}$ .

of 50 Å (open circles) and 400 Å (full circles), respectively: For small values of  $\text{Re}(q'_z)$  the magnitude of  $\epsilon(q'_z)$  depends strongly on the subsurface depth  $\Lambda$ . The most striking feature, however, is the maximum of  $\epsilon(q'_z)$  at  $\text{Re}(q'_z) = 0.037 \text{ \AA}^{-1}$  (as observed for  $\alpha_i = 0.8\alpha_c$ ), corresponding to  $\lambda^* = 100 \text{ \AA}$  as a preferred length scale in the initial  $\Psi_3$ -ordering process perpendicular to the surface. This is a strong indication for an antiphase domain pattern which has been created in an early time spinodal process as sketched in fig. 1.

The second quantity characterizing this transient phenomenon is the relaxation time  $\tau_R$  to the equilibrium intensity value. As can be seen from fig. 2, the decay follows an exponential and  $\tau_R$  depends strongly on the momentum transfer. Overshooting on small length scales vanishes very fast while overshooting on mesoscopic length scales is much more persistent. The inset of fig. 5 shows that  $\tau_R$  is independent of the scattering depth and scales as  $\tau_R \sim \lambda^\alpha$ , with  $\alpha = 1.92$ . In contrast to the bulk where the Lifshitz-Allen-Cahn growth of the average domain size  $L(t)$  is monitored via the FWHM of the associated superstructure reflection, we observe here the disappearance of antiphase domain boundaries in the early-stage coarsening process via surface-diffusion associated with a non-conserved order parameter [17].

To our knowledge there has been no clear-cut experimental confirmation of spinodal processes on lattice systems, while experiments on polymer systems gave evidence for a spinodal mechanism in surface-directed phase separation processes [18]. Bulk X-ray studies of the initial relaxation of (isotropic) short-range order fluctuations in  $\text{Cu}_3\text{Au}$  and  $\text{Fe}_3\text{Al}$  indicate overshooting effects, although the data have not been analyzed for their wave number dependence [6, 19]. Here, we found direct evidence for a spinodal origin of the resulting antiphase domain pattern.

In the bulk of the  $\text{Cu}_3\text{Au}$  system the development of spinodal ordering waves is isotropic with random phases, thus, information about the bulk ordering process is hidden in the isotropic diffuse scattering around the superstructure Bragg positions (incoherent superposition of all ordering waves). In contrast to this, the phases  $\Psi_3(z = 0)$  of the surface-related  $\Psi_3$ -ordering waves described here are pinned by the surface segregation of Au (see fig. 1). Therefore, the “ $\Psi_3$ -scattering” from the surface is coherent, giving rise to Bragg-like in-plane intensity distributions and allowing direct experimental observation of details of the ordering process [20] on small time scales.

We want to point out an interesting aspect of these observations: In a recent Monte Carlo study of the early-time development of (bulk) ordering processes [21] transient overshooting of the local order has been reported for different classes of systems which has been related to transient high local domain order. In the Monte Carlo study transient disorder localized in the domain boundaries network which is balancing the high local domain order dissolves preferentially into the small domains during the coarsening process. Thereby, the domain size is increased while the average order in the growing domains is lowered. In the coarsening process the overshooting local domain order should, therefore, vanish first for small length scales in agreement with our experimental findings.

Notice that we apparently observe here a subtle interplay between energy- and entropy-driven relaxation processes: after the quench into the unstable regime the equilibration of the internal energy involves only the rearrangement of neighbouring atoms and is thus a rather rapid process. The entropy relaxation involves the entire ensemble and is, thus, more sluggish allowing by this a short-time overshooting of local order.

In conclusion, we have studied by evanescent *in situ* line shape analysis the temporal behaviour of parallel and perpendicular ordering waves in the subsurface region of  $\text{Cu}_3\text{Au}(001)$  in two different growth regimes. Our main observation is an unusual temporal behaviour of the perpendicular short-wavelength order fluctuations which relaxes fast and exhibits close

to or within the bulk spinodal regime an unexpectedly large degree of overshooting on an extended spectrum of wave vectors. From the analysis of the wave-number-dependent degree of overshooting, we deduce a dominant length of about 100 Å in the early time ordering process. The subsequent decay of the overshooting order is characterized by the relaxation time  $\tau_R$  which scales as  $\tau_R \sim \lambda^2$  pointing to an ordering process which is governed by surface-diffusion processes from the antiphase boundary network created by a spinodal ordering process.

\* \* \*

The NSLS is supported by DOE under Contract No. DE-AC02-98CH10886. One of us (IKR) is supported by DOE through grant DEFG02-96ER45439.

#### REFERENCES

- [1] GUNTON J. D., SAN MIGUEL M. and SAHNI P. S., in *Phase Transitions and Critical Phenomena*, edited by C. DOMB and J. L. LEBOWITZ, Vol. **8** (Academic Press, London) 1983.
- [2] KOMURA S. and FURUKAWA H. (Editors), *Dynamics of Ordering Processes in Condensed Matter*, (Plenum Press, New York) 1988.
- [3] K. BINDER, in *Materials Science and Technology*, Vol. **V: Phase Transitions in Materials**, P. HAASEN (Editor), (VCH, Weinheim) (1991).
- [4] BRAY A. J., *Adv. Phys.*, **43** (1994) 357.
- [5] CAHN J. W., *Acta Metall.*, **9** (1961) 795; CAHN J., *Acta Metall.*, **10** (1962) 179; HILLIARD J. E., in *Phase Transformations*, edited by H. I. ARONSON (American Society for Metals, Metals Park, Ohio) 1970; COOK H. E., *Acta Metall.*, **18** (1970) 297.
- [6] LUDWIG K. F. *et al.*, *Phys. Rev. Lett.*, **61** (1988) 1859.
- [7] NAGLER S. E. *et al.*, *Phys. Rev. Lett.*, **61** (1988) 718; SHANNON R. F. *et al.*, *Phys. Rev. B*, **46** (1992) 40.
- [8] LAI Z. W., *Phys. Rev. B*, **41** (1990) 9239.
- [9] REICHERT H. *et al.*, *Phys. Rev. Lett.*, **74** (1995) 2006; REICHERT H. and DOSCH H., *Surf. Sci.*, **345** (1996) 27.
- [10] DOSCH H. *et al.*, *Phys. Rev. Lett.*, **60** (1988) 2382.
- [11] REICHERT H. *et al.*, *Phys. Rev. Lett.*, **78** (1997) 3475.
- [12] FISCHER H. P., REINHARD J., DIETERICH W. and MAJHOFFER A., *Europhys. Lett.*, **46** (1999) 755.
- [13] DOSCH H., *Critical Phenomena at Surfaces and Interfaces*, *Springer Tracts Mod. Phys.*, Vol. **126** (Springer) 1992.
- [14] CHEN H. *et al.*, *J. Phys. Chem. Solids*, **38** (1977) 855.
- [15] ASTA M. *et al.*, *Phys. Rev. Lett.*, **66** (1991) 1798.
- [16] The steep initial increase of the intensity is partly due to the initial relaxation of the lattice parameter.
- [17] FURUKAWA H., *Phys. Lett. A*, **97** (1983) 346.
- [18] JONES R. A. L. *et al.*, *Phys. Rev. Lett.*, **66** (1991) 1326.
- [19] PARK B. *et al.*, *Phys. Rev. Lett.*, **68** (1992) 1742.
- [20] Note the particular role of surface roughness: Any notable surface roughness will randomize the  $\Psi_3$ -phase along lateral directions and should destroy the overshooting. For this study the surface has been kept almost perfectly smooth with terraces of typically 1000 Å (see [10]).
- [21] GILHOJ H. *et al.*, *Phys. Rev. Lett.*, **75** (1995) 3305.